

## ARTICLE



# Nuclear expression of AFF2 C-terminus is a sensitive and specific ancillary marker for *DEK::AFF2* carcinoma of the sinonasal tract

Ying-Ju Kuo<sup>1,2</sup>, James S. Lewis Jr.<sup>3,4</sup>, Tra Truong<sup>5,6</sup>, Yi-Chen Yeh<sup>1,2,7</sup>, Rebecca D. Chernock<sup>8</sup>, Changwen Zhai<sup>9</sup>, Yun-An Chen<sup>10</sup>, Takahiro Hongo<sup>11</sup>, Chien-Kuan Lee<sup>12</sup>, Qiuying Shi<sup>13</sup>, Jaylou M. Velez Torres<sup>14</sup>, Ariana B. Geromes<sup>15</sup>, Ying-Hsia Chu<sup>16</sup>, Min-Shu Hsieh<sup>17,18</sup>, Hidetaka Yamamoto<sup>11</sup>, Ilan Weinreb<sup>5,19</sup> and Jen-Fan Hang<sup>1,2,20</sup>✉

© The Author(s), under exclusive licence to United States & Canadian Academy of Pathology 2022

*DEK::AFF2* carcinoma of the sinonasal tract is an emerging entity. The tumor is typically characterized by papillary proliferation of non-keratinizing squamous epithelial cells with monotonous cytologic features, which may mimic other sinonasal tumors. The confirmation of this gene fusion has thus far relied solely on next-generation sequencing, fluorescence in situ hybridization (FISH), or reverse transcription polymerase chain reaction (RT-PCR). This current study aimed to validate an immunohistochemical assay for AFF2 C-terminus as an ancillary marker. We first analyzed publicly available RNA sequencing data of sinonasal tumors from the national center for biotechnology information (NCBI) sequence read archive and identified 3 *DEK::AFF2* carcinomas out of 28 sinonasal tumors. The gene expression of *AFF2* was significantly higher in the fusion-positive cases compared to the wild-type tumors ( $p < 0.001$ ), while *DEK* was not. We then optimized an immunohistochemical assay with an anti-AFF2 C-terminus antibody for ancillary diagnosis. Seventeen *DEK::AFF2* carcinomas, including 11 cases with predominantly low-grade morphology and one showing glandular differentiation, as well as 78 *DEK* FISH-negative sinonasal tumors were evaluated by AFF2 immunohistochemistry (IHC). Sixteen of the 17 *DEK::AFF2* carcinomas showed nuclear AFF2 expression in  $\geq 30\%$  of tumor cells, including one decalcified case that failed FISH and RT-PCR confirmation. The one case that was negative for AFF2 IHC in the tumor cells also lacked expression in the internal positive control. It was thus considered a failure of the IHC rather than a truly negative case and was excluded from the statistical analysis. All *DEK* FISH-negative sinonasal tumors were negative for nuclear AFF2 expression. The nuclear expression of AFF2 IHC showed 100% sensitivity and specificity for *DEK::AFF2* carcinoma. Accordingly, AFF2 IHC is a highly sensitive and specific ancillary marker that distinguishes *DEK-AFF2* carcinoma from the other sinonasal tumors with overlapping morphological features and may be an especially useful alternative for decalcified specimens.

*Modern Pathology* (2022) 35:1587–1595; <https://doi.org/10.1038/s41379-022-01117-4>

## INTRODUCTION

*DEK::AFF2* carcinoma is an emerging entity in the sinonasal tract, middle ear, and skull base<sup>1–5</sup>. The *DEK::AFF2* fusion-derived peptides were shown to stimulate T cell activation through binding to certain patient-specific human leukocyte antigens, which may explain exceptional response to immune checkpoint inhibitor therapy and highlights the potential clinical importance to identify tumors with *DEK::AFF2* fusions<sup>1</sup>. The histomorphologic

spectrum includes nonkeratinizing squamous cell carcinomas (NKSCC) and rarely adenosquamous carcinomas (ADSC)<sup>4,5</sup>. The tumor is characterized by papillary proliferation and inverted growth of basaloid to nonkeratinizing squamous epithelial cells with monotonous cytology, peripheral palisading, acantholytic (discohesive) change, and dense neutrophilic infiltrates<sup>4,5</sup>. The above features may mimic other tumors, especially various types of sinonasal papilloma (SP) and its associated malignancy. To

<sup>1</sup>Department of Pathology and Laboratory Medicine, Taipei Veterans General Hospital, Taipei, Taiwan. <sup>2</sup>School of Medicine, National Yang Ming Chiao Tung University, Taipei, Taiwan. <sup>3</sup>Department of Pathology, Microbiology, and Immunology, Vanderbilt University Medical Center, Nashville, TN, USA. <sup>4</sup>Department of Otolaryngology – Head and Neck Surgery, Vanderbilt University Medical Center, Nashville, TN, USA. <sup>5</sup>Department of Pathobiology and Laboratory Medicine, University of Toronto, Toronto, ON, Canada. <sup>6</sup>Department of Anatomic Pathology, Sunnybrook Health Sciences Centre, Toronto, ON, Canada. <sup>7</sup>Institute of Biomedical Informatics, National Yang Ming Chiao Tung University, Taipei, Taiwan. <sup>8</sup>Department of Pathology and Immunology, Washington University in St. Louis, St. Louis, MO, USA. <sup>9</sup>Department of Pathology, Eye, Ear, Nose and Throat Hospital, Fudan University, Shanghai, China. <sup>10</sup>Department of Pathology and Laboratory Medicine, Taichung Veterans General Hospital, Taichung, Taiwan. <sup>11</sup>Department of Anatomic Pathology, Graduate School of Medical Sciences, Kyushu University, Fukuoka, Japan. <sup>12</sup>Department of Pathology, Kuang Tien General Hospital, Taichung, Taiwan. <sup>13</sup>Department of Pathology, Emory University, Atlanta, GA, USA. <sup>14</sup>Department of Pathology and Laboratory Medicine, University of Miami Miller School of Medicine, Miami, FL, USA. <sup>15</sup>Anatomic and Clinical Laboratory Associates, P.C, Nashville, TN, USA. <sup>16</sup>Department of Pathology, Chang Gung Memorial Hospital and Chang Gung University, Taoyuan, Taiwan. <sup>17</sup>Department of Pathology, National Taiwan University Hospital and National Taiwan University College of Medicine, Taipei, Taiwan. <sup>18</sup>Graduate Institute of Pathology, National Taiwan University College of Medicine, Taipei, Taiwan. <sup>19</sup>Laboratory Medicine Program, University Health Network, Toronto, ON, Canada. <sup>20</sup>Institute of Clinical Medicine, National Yang Ming Chiao Tung University, Taipei, Taiwan. ✉email: jfhang@vghtpe.gov.tw

Received: 11 March 2022 Revised: 18 May 2022 Accepted: 23 May 2022  
Published online: 14 June 2022

distinguish the *DEK::AFF2* carcinoma from its mimickers is a diagnostic challenge and molecular confirmation is mandatory. In previous studies, the gene fusion testing relied solely on RNA-based next-generation sequencing (NGS), fluorescence in situ hybridization (FISH), or reverse transcription polymerase chain reaction (RT-PCR)<sup>1–5</sup>. However, these molecular tests are neither available nor cost-effective in most laboratories. A surrogate immunohistochemistry (IHC)-based marker for *DEK::AFF2* fusion would be much more useful for routine pathological diagnosis.

The *DEK* gene on chromosome 6p22.3 is a proto-oncogene that encodes DEK nuclear protein which binds to DNA with the SAP domain<sup>6</sup>. Transcriptional upregulation of *DEK* has been found in various cancer types<sup>7–9</sup>, including head and neck cancer. Immunohistochemical expression of DEK protein has also been reported in 64–100% of head and neck squamous cell carcinomas (SCCs)<sup>10–12</sup>. The *AFF2* gene on chromosome Xq28 is associated with the fragile X E (FRAXE) syndrome. The encoded AFF2 protein is a nuclear transcriptional activator that binds to RNA through its C-terminal domain and is usually localized in nuclear speckles<sup>13</sup>. The overexpression of AFF2 has never been reported in head and neck cancers before. The fusion between *DEK* exon 7 and multiple breakpoints in *AFF2*, including exon 4, 5, 6, and 9, expectedly results in the translation of *DEK::AFF2* chimeric proteins<sup>4</sup>. The chimeric proteins carrying the major functional domains, the SAP domain of DEK on the N-terminus and the C-terminal domain of AFF2 on the C-terminus, are presumably overexpressed resulting in tumorigenesis. Given the overexpression of DEK in most head and neck SCCs, AFF2 is potentially a more specific target for IHC detection of *DEK::AFF2* carcinoma.

This study aimed to demonstrate the differential gene expression of *DEK* and *AFF2* among sinonasal tumors using publicly available RNA sequencing (RNAseq) data and to validate an anti-AFF2 C-terminus antibody as an ancillary immunohistochemical marker for the diagnosis of *DEK::AFF2* carcinoma.

## MATERIAL AND METHODS

### RNA sequencing data mining

To evaluate the incidence of *DEK::AFF2* fusion and the differential gene expression among SPs and carcinomas, we searched the literature on PubMed using the keywords “sinonasal papilloma OR sinonasal carcinoma AND RNAseq” for studies with available RNAseq data to the public. Fusion detection was performed using the FusionMap bioinformatics tool<sup>14</sup> and was filtered for in-frame and canonical fusions. The RNA sequences of the samples with detected *DEK::AFF2* fusion were visualized on the Integrative Genomics Viewer software (version 2.8.3, The Broad Institute, Cambridge, MA, USA)<sup>15</sup>. The RNA reads were aligned to the reference genome (GRCh38) by STAR<sup>16</sup>, and then converted to fragments per kilobase of exon model per million reads mapped (FPKM) unit using HTSeq and customized R script<sup>17</sup>. The gene expression level of *DEK* and *AFF2* were compared among the samples with or without *DEK::AFF2* fusion.

### Case selection

The study has been approved by the institutional review board (IRB) of Taipei Veterans General Hospital (IRB no.: 2020-12-012CC) and the other participant institutions. The *DEK::AFF2* carcinomas were collected from the surgical pathology archives of Taipei Veterans General Hospital and from all of the various authors' archives and consultation files. The *DEK::AFF2* fusion was confirmed by either FISH and/or RT-PCR<sup>4</sup> or NGS<sup>2</sup>. The clinical information was obtained from the medical records. The histomorphology was reviewed in details by two pathologists specialized in head and neck pathology (YJK and JFH).

A collection of *DEK::AFF2* fusion-negative sinonasal tumors with morphologic overlap was selected through multi-institutional collaboration as IHC controls. These included inverted papilloma (IP), oncocytic papilloma (OP), SCC ex-IP, SCC ex-OP, NKSCC including low-grade papillary Schneiderian carcinomas (LGPSC), keratinizing SCC, ADSC, poorly-differentiated carcinoma including sinonasal undifferentiated carcinoma, *NUT* carcinoma, *SMARCB1*-deficient sinonasal carcinoma, human papillomavirus (HPV)-related multiphenotypic sinonasal carcinoma (HMSC),

nasopharyngeal carcinoma (NPC), teratocarcinosarcoma, non-intestinal type adenocarcinoma, adamantinoma-like Ewing sarcoma (AES), olfactory neuroblastoma, alveolar rhabdomyosarcoma, and ectopic pituitary adenoma. All control cases were evaluated for *DEK::AFF2* fusion by *DEK* FISH as previously described<sup>4</sup>. Several morphologic features, including exophytic pattern, broad papillae, thin papillae, inverted growth pattern, anastomosing labyrinth-like trabeculae, acantholytic change, monotonous cytomorphology, and neutrophilic infiltrates were reviewed for the *DEK* fusion-negative SCCs ex-SP and NKSCCs to compare with the *DEK::AFF2* carcinomas.

### AFF2 immunohistochemistry

The AFF2 IHC using an anti-AFF2 C-terminus antibody against a.a.715-855 (HPA003139, dilution 1:100, Sigma-Aldrich, St. Louis, MO, USA) was optimized on a BenchMark ULTRA system (Ventana, Tucson, AZ, USA) using a selection of normal control tissues, including tonsil, salivary gland, pancreas, placenta, cerebellum, and testis, as well as *DEK::AFF2* carcinoma specimens. The automatic staining protocol consisted of deparaffinization, antigen retrieval with ULTRA CC1 (Ventana) at 100 °C for 32 min, primary antibody incubation at 36 °C for 2 h, OptiView HQ Linker (Ventana) for 8 min, OptiView HRP Multimer (Ventana) for 8 min, OptiView Amplification kit (Ventana) for 8 min, and counterstaining with hematoxylin for 24 min. Four-micrometer formalin-fixed paraffin-embedded (FFPE) sections of the *DEK::AFF2* carcinomas and the control cases were used for the IHC. The staining intensity (weak, moderate, or strong), percentage of stained tumor cells, and staining localization (nuclear or cytoplasmic) were recorded. Nuclear expression of any intensity in  $\geq 30\%$  of the tumor cells was regarded as positive staining.

### Statistical analysis

The means of RNA expression levels between two groups were compared using Wilcoxon tests. For the performance of AFF2 IHC in the diagnosis of *DEK::AFF2* carcinoma, test sensitivity, specificity, and predictive values were analyzed. The histomorphology between *DEK::AFF2* carcinomas and *DEK* FISH-negative tumors, with a focus on SCC ex-SP and NKSCC, were compared using Fisher exact tests. Statistical analyses were performed using R statistical software version 4.1.2 (R Foundation for Statistical Computing, Vienna, Austria). Two-tailed *p* values < 0.05 were regarded statistically significant.

## RESULTS

### DEK::AFF2 fusion detection in archived RNA sequencing data

Four published studies were identified on PubMed using the keywords (last accession date: November 26th, 2021). Among them, one study had RNAseq data that can be downloaded from the national center for biotechnology information (NCBI) sequence read archive (Reference No.: PRJNA507589)<sup>18</sup>. The study cohort consisted of consecutive patients of 14 SPs, 14 sinonasal SCCs, and 4 normal sinonasal mucosa specimens. We performed fusion detection on the archived RNAseq data of all 28 tumor samples using the FusionMap bioinformatics tool. *DEK::AFF2* fusion was identified in three cases (3/28, 10.7%), including two classified as IPs with carcinoma in situ (TC17 and TC19) and one classified as NKSCC (TS05) by the original investigators. The former two cases showed *DEKex7::AFF2ex5* fusion with *DEKex7::AFF2ex6* alternative splicing transcripts and the latter showed *DEKex7::AFF2ex4* fusion (Fig. 1A, B). The *DEK* and *AFF2* gene expression levels of the fusion-positive cases versus wild-type cases and normal sinonasal mucosa specimens were also analyzed. The *AFF2* gene showed higher RNA expression in the fusion-positive cases compared to wild-type tumors ( $p < 0.001$ ) and normal mucosa specimens ( $p = 0.057$ ) (Fig. 1C), while no significant differences in *DEK* gene expression were noted (Fig. 1D). In addition, the *DEK* gene expression levels of the normal mucosa specimens were significantly higher than *AFF2* (median: 1.610 versus 0.034,  $p = 0.029$ ), suggesting that the *DEK* gene may drive the overexpression of *AFF2* in the *DEK::AFF2* fusion-positive tumors since it is on the 5'-side. Therefore, we hypothesized that *AFF2* overexpression could be detected by an IHC assay targeting the

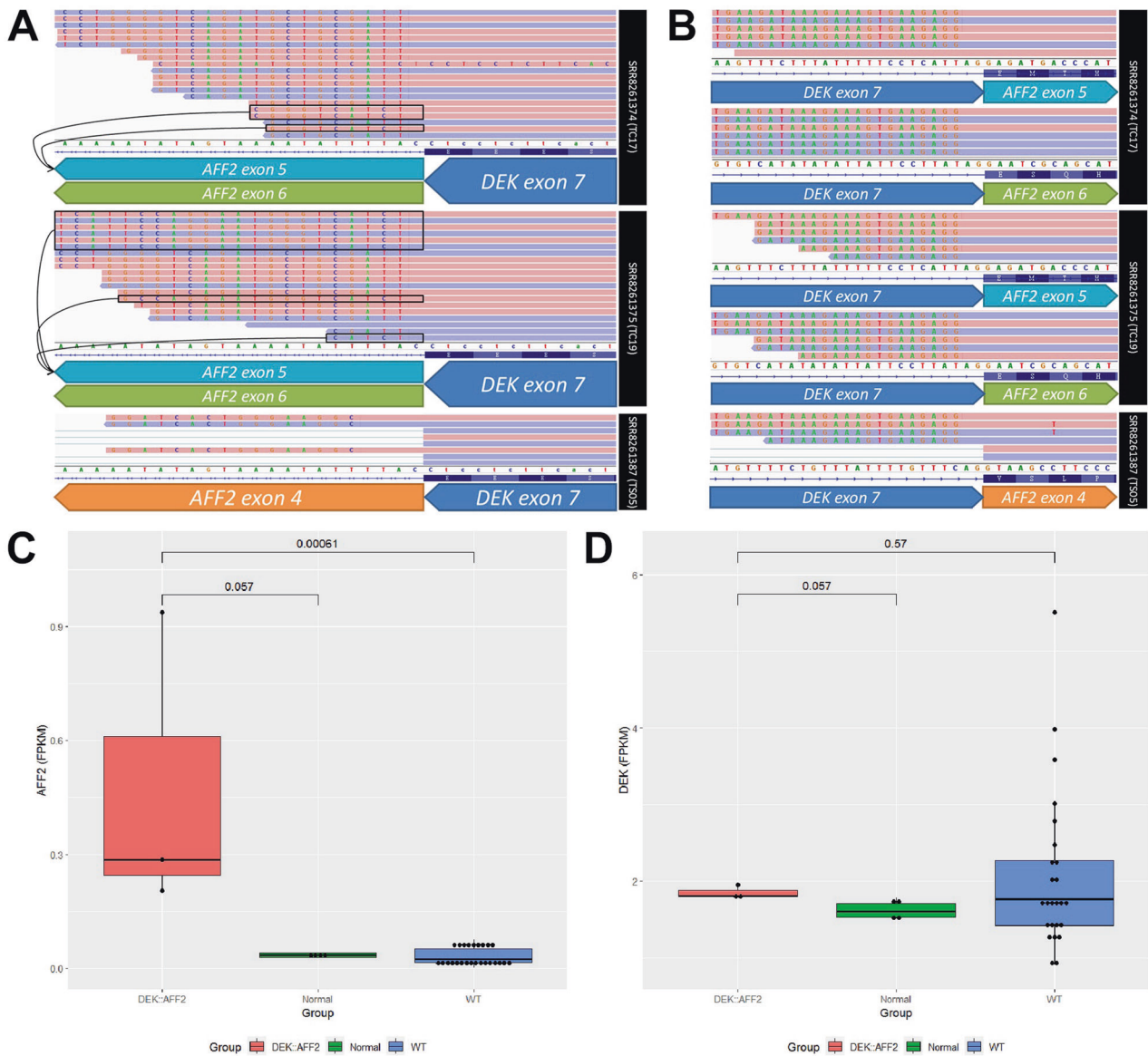


**Fig. 1 RNA sequencing data mining.** Integrative Genomics Viewer visualization of the three cases with *DEK::AFF2* fusions on both (A) *DEK* and (B) *AFF2* genes. Cases TC17 and TC19 showed *DEKex7::AFF2ex5* fusion with *DEKex7::AFF2ex6* alternative splicing transcripts and case TS05 showed *DEKex7::AFF2ex4* fusion. Gene expression levels of (C) *AFF2* and (D) *DEK* genes among the *DEK::AFF2* fusion-positive tumors, wild-type (WT) tumors, and normal sinonasal mucosal specimens. The *AFF2* expression levels of the *DEK::AFF2* fusion-positive tumors were significantly higher than the WT tumors ( $p = 0.00061$ ), while no significant differences were noted for the other comparisons. FPKM fragments per kilobase of exon model per million reads mapped.

*AFF2* C-terminus peptides on the FFPE tumor sections. The chimeric fusion protein may go into the tumor nuclei given the SAP DNA-binding domain on the N-terminus, nuclear localization sequences, and nuclear speckle-binding C-terminal domain, resulting in nuclear expression of the IHC (Fig. 2).

**Collected *DEK::AFF2* carcinomas and controls**

We collected 17 *DEK::AFF2* carcinomas. The clinicopathologic features are summarized in Table 1. Nine cases had been reported in previous studies (case 1–7<sup>4</sup> and case 13–14<sup>2</sup>). There were nine females and eight males with a median age of 61 years (range: 28–79 years). The sites of the initial presentation included the nasopharynx, nasal cavity, paranasal sinuses, skull base, and/or lacrimal sac. The original diagnoses included 5 SP, 5 SP with dysplasia/carcinoma in situ, 1 atypical papillary epithelial proliferation, 1 NKSCC, 1 poorly-differentiated SCC, 1 SCC, 1 undifferentiated

type NPC, 1 ciliated ADSC, and 1 *DEK::AFF2* carcinoma. In total, 11 of the 17 cases were initially diagnosed as benign lesions. The follow-up data were available for all cases and the median follow-up time was 18 months (range: 1 month–18 years). Ten patients (58.8%) showed no evidence of disease, six (35.3%) were alive with disease, and only one (5.9%) died of disease. One or more local recurrences had been recorded in nine cases (52.9%). Three cases (case 4, 6, and 14; 17.6%) developed nodal metastases. One case (case 14; 5.9%) had proven lung metastases and the disease stabilized under chemotherapy. One case (case 4; 5.9%) had a widely invasive tumor through multiple recurrences and eventually succumbed to the disease 18 years after the initial diagnosis.

Morphologically, all *DEK::AFF2* carcinomas had inverted thin trabeculae which interconnected to each other and formed a complex maze-like appearance, thin and delicate papillae, and a very monotonous appearance. Most cases showed acantholytic

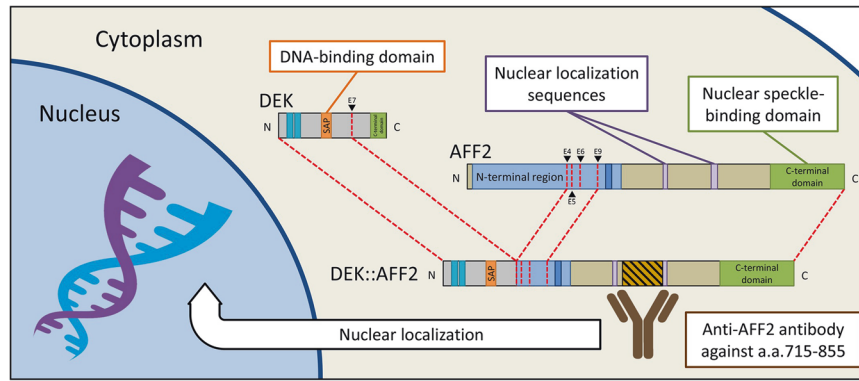


**Fig. 2** Illustration of the AFF2 immunohistochemistry detection of the DEK::AFF2 fusion protein. The anti-AFF2 antibody against the AFF2 C-terminus peptides (a.a. 715–855) binds to the DEK::AFF2 fusion protein, which goes into the tumor nuclei given the SAP DNA-binding domain on the N-terminus, nuclear localization sequences, and nuclear speckle-binding C-terminal domain.

**Table 1.** Clinicopathologic features of *DEK::AFF2* carcinoma.

Case No.	Age	Sex	Location	Original diagnosis	Treatment	FU interval	Disease status
1.	61	F	NP, NC	SP with dysplasia	Excision + CCRT	7 m	NED
2.	79	F	NC	SP with dysplasia	Excision	55 m	AWD
3.	28	M	FS, ES	SP with CIS	Excision + RT	26 m	NED
4.	47	F	ES	SP	Wide excision + ND + CCRT	18 y	DOD
5.	64	M	NC	SP with CIS	Excision	10 m	NED
6.	53	F	NC, NP, SB	SP	Excision + RT	18 m	AWD
7.	51	F	NC	SP	Excision + RT	30 m	NED
8.	77	M	Ear, SB	SP with CIS	Excision	8 m	NED
9.	68	F	NC	Atypical papillary proliferation	Excision	13 m	AWD
10.	72	M	NC, SB	SP	Excision + RT	20 m	NED
11.	73	F	NC	Ciliated ADSC	Excision	17 m	NED
12.	68	F	NC	Nonkeratinizing SCC	Excision + CCRT	39 m	NED
13.	46	M	NP, SB	Poorly differentiated SCC	Excision + RT	46 m	AWD
14.	68	M	SB, EAC	SCC	Excision + CCRT	27 m	AWD
15.	54	F	LS	SP	Excision	9 m	NED
16.	60	M	NC	Undifferentiated NPC	Excision + RT	3 m	AWD
17.	31	M	NC	<i>DEK::AFF2</i> carcinoma	Excision	1 m	NED

NP nasopharynx, NC nasal cavity, FS frontal sinus, ES ethmoid sinus, EAC external auditory canal, SB skull base, LC lacrimal sac, SP sinonasal papilloma, CIS carcinoma in situ, SCC squamous cell carcinoma, NPC nasopharyngeal carcinoma, ADSC adenosquamous carcinoma, RT radiotherapy, CT chemotherapy, CCRT concurrent chemoradiotherapy, ND neck dissection, NA not available, FU follow-up, m month, y year, NED no evidence of disease, AWD alive with disease, DOD died of disease.

change (16/17, 94.1%), prominent neutrophilic infiltrates (14/17, 82.4%), and broad papillae (13/17, 76.5%). Eleven cases were relatively bland looking and lack infiltrative pattern, which resembled tumors that have been described as LGPSCs (Fig. 3A, B). Five cases were infiltrative and had tumor necrosis, and/or diffuse high-grade cytology (Fig. 3C, D). One case had a predominant NKSCC component with several foci of ciliated glandular formation (Fig. 3E) and aggregates of goblet-like mucous cells (Fig. 3F). Molecular confirmation using FISH and RT-PCR failed in one case (case 12) due to tissue decalcification and poor nucleic acid quality, and the diagnosis was based on the typical histomorphology and positive AFF2 IHC.

A total of 78 *DEK* FISH-negative sinonasal tumors were selected for IHC control, including 8 IPs, 2 OPs, 6 SCCs ex-IP, 1 SCC ex-OP, 26 NKSCCs (including 5 LGPSCs), 6 keratinizing SCCs, 9 ADSCs, 6 poorly-differentiated carcinomas, 3 *NUT* carcinomas, 2 *SMARCB1*-deficient sinonasal carcinomas, 2 HMSCs, 1 undifferentiated type NPC, 1 teratocarcinoma, 1 non-intestinal type adenocarcinoma, 1 AES,

1 olfactory neuroblastoma, 1 alveolar rhabdomyosarcoma, and 1 ectopic pituitary adenoma. Among the *DEK* FISH-negative tumors, some shared overlapping morphologic features with the *DEK::AFF2* carcinomas. Detailed morphologic comparison between *DEK::AFF2* carcinoma and a selection of *DEK* FISH-negative sinonasal carcinoma, excluding entities with commonly available diagnostic IHC, such as *INI-1*, *NUT*, and *NKX2.2*, was performed (Table 2). While exophytic pattern, broad papillae, and inverted growth pattern were also commonly seen in *DEK* FISH-negative SCC ex-SP and NKSCC, thin papillae ( $p = 0.020$ ), anastomosing labyrinth-like trabeculae ( $p < 0.001$ ), acantholytic change ( $p = 0.004$ ), monotonous cytology ( $p < 0.001$ ), and neutrophilic infiltrates ( $p = 0.008$ ) were statistically more frequent in the *DEK::AFF2* carcinoma.

#### AFF2 immunohistochemistry

In the normal control tissues, AFF2 IHC showed strong cytoplasmic staining in the plasma cells and serous acinar cells of the salivary gland, and moderate cytoplasmic staining in the pancreatic acinar

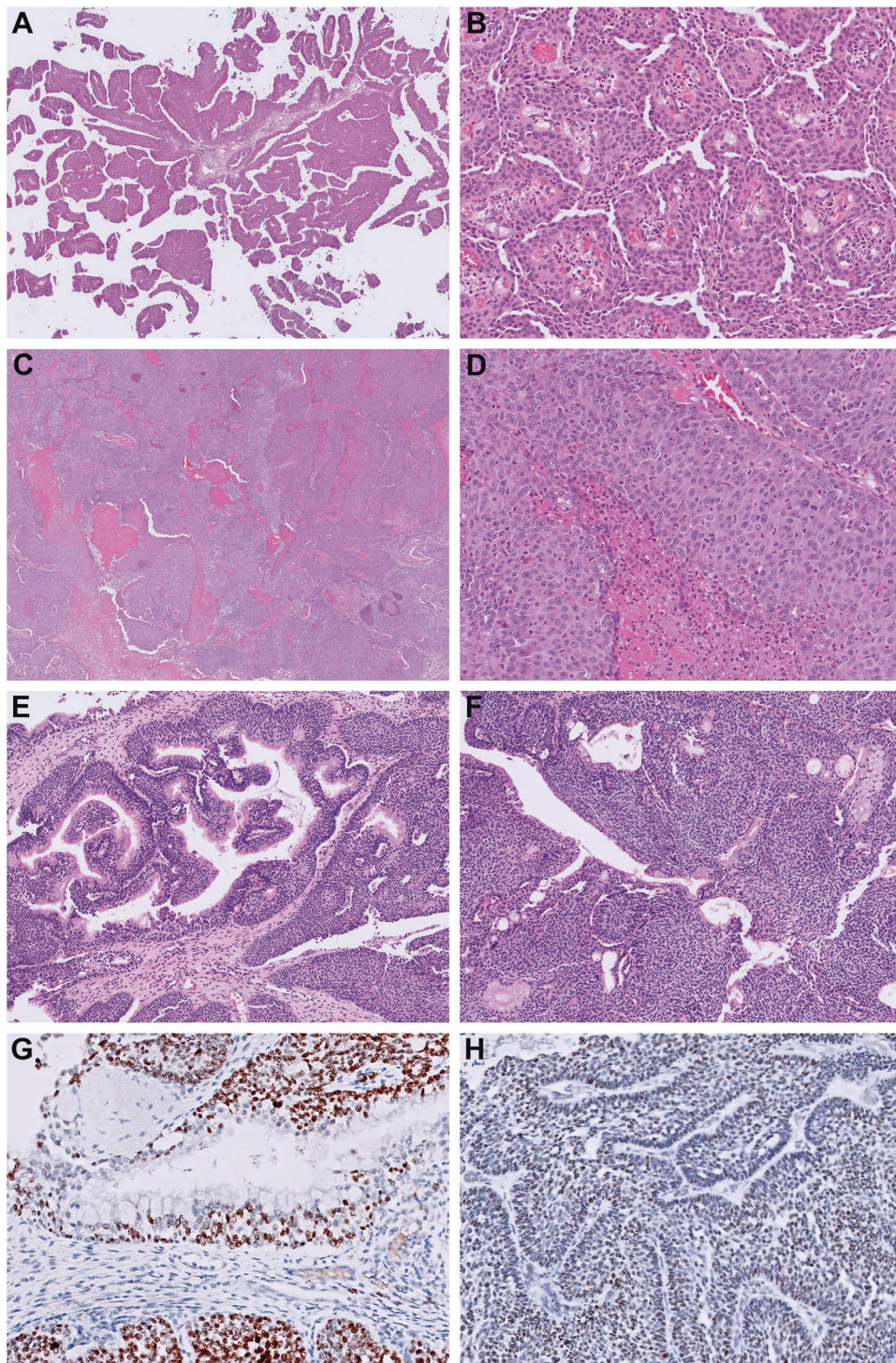


**Fig. 3 Morphologic spectrum of *DEK::AFF2* carcinoma and the *AFF2* immunohistochemistry (IHC).** **A** The low-grade papillary Schneiderian carcinoma-like cases showed predominantly exophytic papillary growth patterns without definitive evidence of stromal invasion (H&E, 20X). **B** The tumor cells were monotonous and bland-looking and showed acantholytic change with pseudopapillary formation (H&E, 200X). **C** The high-grade nonkeratinizing squamous cell carcinoma-like cases had crowded ribbon-like inverted tumor nests with focal necrosis (H&E, 20X). **D** The tumor cells were monotonous but high-grade, which was characterized by nuclear enlargement, vesicular chromatin, and prominent nucleoli (H&E, 200X). **E** The only case (case 11) classified as adenosquamous carcinoma showed a predominant nonkeratinizing squamous cell carcinoma appearance with focal ciliated glandular formation (H&E, 100X). **F** Aggregates of goblet-like mucous cells were also noted (H&E, 100X). **G** Diffuse and strong nuclear staining of *AFF2* IHC, particularly in the ciliated glandular component in case 11 (400X). **H** Moderate nuclear staining of *AFF2* IHC in case 3 (400X).

**Table 2.** Histomorphologic comparison between *DEK::AFF2* carcinoma and *DEK* fusion-negative carcinoma.

	<b><i>DEK::AFF2</i> fusion-associated carcinoma (n = 17)</b>	<b><i>DEK</i> fusion-negative carcinoma<sup>a</sup> (n = 33)</b>	<b>p value</b>
Exophytic pattern	17 (100%)	29 (87.9%)	0.286
Broad papillae	13 (76.5%)	20 (60.6%)	0.351
Thin papillae	17 (100%)	24 (72.7%)	<b>0.020</b>
Inverted growth pattern	17 (100%)	32 (97.0%)	1.000
Anastomosing labyrinth-like trabeculae	17 (100%)	8 (24.2%)	<b>&lt;0.001</b>
Acantholytic change	16 (94.1%)	17 (51.5%)	<b>0.004</b>
Monotonous cytomorphology	17 (100%)	13 (39.4%)	<b>&lt;0.001</b>
Neutrophilic infiltrates	14 (82.4%)	14 (42.4%)	<b>0.008</b>

Bold type suggests statistically significance.

<sup>a</sup>Including squamous cell carcinoma ex-sinonasal papilloma, nonkeratinizing squamous cell carcinoma, and low-grade papillary Schneiderian carcinoma.

**Table 3.** *AFF2* immunohistochemical (IHC) and molecular details of *DEK::AFF2* carcinoma.

Case no	<b><i>AFF2</i> IHC</b>			<b><i>DEK</i> FISH</b>	<b>RT-PCR</b>	<b>NGS</b>
	<b>Intensity</b>	<b>Tumor cell %</b>	<b>Localization</b>			
1.	Strong	75%	Nuclear	+	D7A9	ND
2.	Strong	70%	Nuclear	+	D7A6	ND
3.	Moderate	35%	Nuclear	+	D7A9	ND
4.	Strong	30%	Nuclear	+	D7A4	ND
5.	Strong	95%	Nuclear	+	D7A4	ND
6.	Failed <sup>a</sup>	NA	NA	+	D7A5	ND
7.	Moderate	90%	Nuclear	+	D7A5	ND
8.	Strong	70%	Nuclear	+	D7A4	ND
9.	Strong	90%	Nuclear	+	D7A6	ND
10.	Moderate	90%	Nuclear	+	ND	ND
11.	Strong	60%	Nuclear	+	D7A5	ND
12.	Moderate	70%	Nuclear	Failed <sup>b</sup>	Failed <sup>b</sup>	ND
13.	Strong	90%	Nuclear	ND	ND	D7A6
14.	Moderate	30%	Nuclear	ND	ND	D7A9
15.	Strong	60%	Nuclear	+	ND	ND
16.	Strong	90%	Nuclear	ND	ND	D7A4
17.	Strong	70%	Nuclear	+	D7A5	ND

*FISH* fluorescence in situ hybridization, *NGS* next-generation sequencing, *ND* not done, *NA* not available.

<sup>a</sup>Negative expression in the internal positive control (plasma cells).

<sup>b</sup>Possibly due to decalcification.

cells and the cytotrophoblasts (Supplementary Fig. 1). The details of *AFF2* IHC results and molecular testing for *DEK::AFF2* carcinomas are summarized in Table 3. In the *DEK::AFF2* carcinoma cases, *AFF2* IHC was successfully done on sixteen cases and all of them were positive for nuclear expression with 81.3% (13/16) showed staining in more than 50% of the tumor cells. Focal staining was only noted in three cases, 35% in one and 30% in two. Strong nuclear staining was seen in eleven (Fig. 3G) and moderate staining in five (Fig. 3H). Case 6 showed completely negative nuclear *AFF2* staining in the tumor cells but were also negative for cytoplasmic staining in the adjacent plasma cells as an internal positive control, despite repeated staining. Thus, the IHC result was considered a failure in this case due to possible inadequate tissue preservation and was excluded for statistic analysis. The details of the *AFF2* IHC results and ancillary testing for *DEK* FISH-negative sinonasal tumors are summarized in Table 4. All cases were negative for nuclear expression of *AFF2* IHC (Fig. 4). There were 12 cases (15.4%) that showed focal and weak to moderate nonspecific cytoplasmic

staining in no more than 15% of the tumor cells. Nuclear expression of *AFF2* IHC showed 100% specificity, 100% sensitivity, 100% positive predictive value, and 100% negative predictive value in diagnosing *DEK::AFF2* carcinoma.

## DISCUSSION

*DEK::AFF2* carcinoma of the sinonasal tract and skull base is a newly defined entity characterized by the complex inverted and exophytic growth pattern, acantholytic change, and a prominent infiltrate of neutrophils<sup>2-5</sup>. The tumor cells, either bland or frankly carcinoma-like, have an essentially monotonous appearance, which is typical of a gene fusion-associated tumor. Given the nonkeratinizing tumor cells and mixed exophytic and inverted architecture, the *DEK::AFF2* carcinoma is most likely to be diagnosed as NKSCC or various types of SP with or without malignant transformation in the previous studies<sup>1-5</sup>. *DEK::AFF2* fusion was reported in 21.4% (3/14) and 48.1% (13/27) of selected

**Table 4.** The results of AFF2 immunohistochemistry (IHC) in *DEK* fusion-negative sinonasal tumors.

Tumor type	n	AFF2 IHC	Other ancillary tests	
			IHC & EBER ish	Molecular tests
IP	8	—	ND	<i>EGFR</i> mutation (+)
OP	2	—	ND	<i>KRAS</i> mutation (+)
SCC ex-IP	6	—	ND	ND
SCC ex-OP	1	—	ND	ND
NKSCC	21	—	ND	ND
LGPSC	5	—	ND	High risk HPV (–)
KSCC	6	—	ND	ND
ADSC	9	—	ND	ND
PDC	6	—	No significant findings <sup>a</sup>	High risk HPV (–)
<i>NUT</i> carcinoma	3	—	<i>NUT</i> (+)	ND
<i>SMARCB1</i> carcinoma	2	—	Loss of INI1	ND
HMSC	2	—	P16 (+)	HPV type 33 (+)
NPC	1	—	EBER ish (+)	ND
Teratocarcinosarcoma	1	—	β-catenin (+), BRG1 preserved	ND
NIADC	1	—	CK7 (+) and CK20 (–)	ND
AES	1	—	NKX2.2 (+)	<i>EWSR1</i> FISH (+)
OFNB	1	—	Synaptophysin (+)	ND
ARMS	1	—	Myogenin (+)	<i>FOXO1</i> FISH (+)
EPA	1	—	FSH and LH (+)	ND

IP inverted papilloma, ND not done, OP oncocytic papilloma, SCC squamous cell carcinoma, NKSCC nonkeratinizing SCC, LGPSC low-grade papillary Schneiderian carcinoma, HPV human papillomavirus, KSCC keratinizing SCC, ADSC adenosquamous carcinoma, PDC poorly differentiated carcinoma, *SMARCB1* carcinoma *SMARCB1*-deficient sinonasal carcinoma, HMSC HPV-related multiphenotypic sinonasal carcinoma, NPC nasopharyngeal carcinoma, undifferentiated type, *EBER ish* Epstein-Barr virus-encoded RNA in situ hybridization, NIADC non-intestinal type adenocarcinoma, AES adamantinoma-like Ewing sarcoma, OFNB olfactory neuroblastoma, ARMS alveolar rhabdomyosarcoma, EPA ectopic pituitary adenoma.

<sup>a</sup>*NUT* (–), NKX2.2 (–), EBER ish (–); INI1 and/or BRG1 preserved.

cases of NKSCCs and SPs from the sinonasal tract and skull base in two recent series respectively<sup>4,5</sup>. In the current study, we identified *DEK::AFF2* fusion in 10.7% (3/28) of consecutive samples of SPs and sinonasal SCCs using publicly available RNAseq data. We believe that this percentage approximates the actual incidence of *DEK::AFF2* carcinoma among papillary sinonasal tumors.

In our histomorphologic review, the majority of *DEK::AFF2* carcinomas were relatively bland in morphology and composed predominantly of exophytic papillae (64.7%, 11/17), which were reminiscent of tumors previously described as LGPSCs and may easily be misdiagnosed as an SP. There was only one exceptional ADSC with aggregates of goblet-like mucus cells and glandular structure with focal luminal ciliation, which has never been reported in the literature. The ciliated glandular epithelial cells and goblet cells intermixed well within the tumor proper and were positive for the AFF2 IHC (Fig. 3G), and hence were considered as a neoplastic component. The diagnosis of this case was particularly challenging since the squamous component was papillary and low-grade, and scattered goblet cells and ciliated cells were regarded as the morphologic findings in favor of an IP<sup>5,19</sup>. Rooper et al. also reported one unusual ADSC with *DEK::AFF2* fusion, which was morphologically more high-grade and had overt formation of nonciliated glands with intraluminal mucin<sup>5</sup>. Regarding the clinical behavior, the local tumor recurrence rate was high in 52.9% (9/17) of our cases. However, the rates of lymph node metastasis (17.6%, 3/17), distant metastasis (5.9%, 1/17), and tumor-related death (5.9%, 1/17) were much lower than that reported by Rooper et al.<sup>5</sup>. This might be due to a smaller case number of patients with available follow-up data ( $n = 8$ ) in the prior study and the fact that all of their cases were identified by the NGS, which is likely to be performed in advanced disease for therapeutic guidance.

In this study, we demonstrated that the gene expression of *AFF2* was significantly higher in *DEK::AFF2* carcinomas and the AFF2 IHC was a novel diagnostic marker with high sensitivity and specificity. AFF2 IHC was positive in 100% (16/16) *DEK::AFF2* carcinomas and all displayed moderate to strong nuclear expression in no less than 30% of the tumor tissue. One of these cases had the morphology consistent with that of a *DEK::AFF2* carcinoma but failed for molecular confirmation due to tissue decalcification (case 12). In this case, the AFF2 IHC was expressed in 70% of the tumor cells with moderate immunoreactivity. This suggested that the chimeric fusion protein was more tolerant of tissue processing than DNA/RNA and AFF2 IHC has a potential utility in specimens that are inadequate for nucleic acid-based testing. The AFF2 IHC also stained the cytoplasm of plasma cells and non-neoplastic serous acinar cells of the salivary glands. These normal components are frequently present in sinonasal biopsies and conveniently serve as internal positive controls. In contrast, the 78 *DEK* FISH-negative sinonasal tumors were all negative for nuclear expression of *AFF2* by IHC. The overall sensitivity, specificity, positive predictive value, and negative predictive value of the nuclear expression of AFF2 IHC were 100%, 100%, 100%, and 100% respectively. The above results suggest that AFF2 IHC is a highly sensitive and specific ancillary marker for the diagnosis of *DEK::AFF2* carcinoma and appears to work properly even in acid decalcified specimens.

The differential diagnosis of *DEK::AFF2* carcinoma includes a variety of tumors, especially SP and its associated dysplasia/malignancy and NKSCC (including LGPSC). Given the bland morphology in most *DEK::AFF2* carcinomas, IP with dysplasia is probably the most challenging differential. The morphologic clues rely on the character of the inverted nests, which are consistently

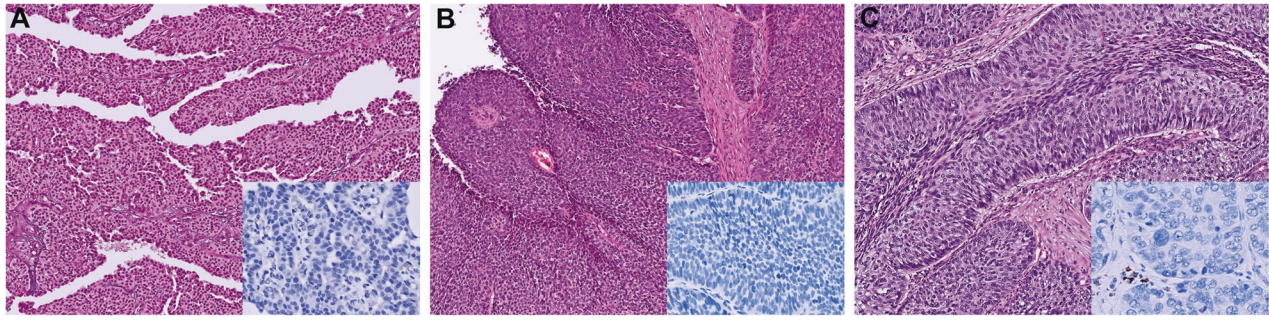


**Fig. 4 Morphology and AFF2 immunohistochemistry (IHC) of the *DEK* fluorescence in situ hybridization-negative sinonasal tumors (H&E, 200X; inset: AFF2 IHC, 400X). A** Low-grade papillary Schneiderian carcinoma had thin and delicate papillary structures lined by uniform and bland tumor cells, which were negative for AFF2 IHC. **B** Nonkeratinizing squamous cell carcinoma consisted of nonkeratinizing to basaloid tumor cells showing exophytic and endophytic growth patterns. AFF2 IHC was negative. **C** The squamous cell carcinoma (SCC) component in an SCC ex-inverted papilloma (IP) showed inverted trabeculae with vague peripheral palisading. AFF2 IHC only highlighted a few plasma cells in the stroma as the internal positive control.

rounded with central lumen formation in IP rather than relatively angular and labyrinth-like in *DEK::AFF2* carcinoma<sup>4</sup>. Besides, most *DEK::AFF2* carcinomas have only one cell type, rather than a mixture of squamous, ciliated respiratory, and goblet cells. LGPSC is also characterized by the bland morphology simulating an SP<sup>19,21</sup>. It does not have the mutations typical for SPs<sup>19,21</sup> and was found to harbor *DEK::AFF2* fusion in a subset of cases<sup>4,5</sup>. In this current study, we found that the majority of sinonasal tumors showing features of LGPSC had *DEK::AFF2* fusion (68.6%, 11/16), therefore highlighting the importance of *DEK::AFF2* fusion testing in cases with features of LGPSC. Whether there are any specific genetic alterations in the *DEK* FISH-negative LGPSCs awaits further investigation. In 2017 WHO classification, sinonasal NKSCC is characterized by anastomosing tumor ribbons with pushing borders eliciting a minimal desmoplastic reaction<sup>22</sup>. In addition to high-risk HPV and preceding SP<sup>23–26</sup>, genetic fusions such as *DEK::AFF2*<sup>1–5</sup> and *ETV6::TNFRSF8*<sup>27</sup> were recently identified in tumors showing NKSCC morphology. These findings suggest that sinonasal NKSCC contains diverse molecular alterations and might include a subset of cases that could be further classified into other distinct entities. Despite the morphologic similarity, we demonstrated that labyrinth-like trabeculae, monotonous cytomorphology, acantholytic change, neutrophilic infiltrates, and thin papillae were the morphologic features significantly associated with *DEK::AFF2* carcinoma compared to *DEK* FISH-negative SCCs ex-SP and NKSCC.

Sinonasal ADSC is rare and yet to be delineated in the literature. In addition to the *DEK::AFF2* ADSC, high-risk HPV-related sinonasal carcinoma and basaloid type *SMARCB1*-deficient sinonasal carcinoma were also reported to show occasional glandular differentiation<sup>23,28</sup>. Other sinonasal tumors showing monotonous appearance, papillary growth, and/or inverted nests may also mimic *DEK::AFF2* carcinoma (supplementary Fig. 2). *NUT* carcinoma and AES are typically monotonous given their fusion-associated nature<sup>29,30</sup>. Prominent exophytic architecture is occasionally seen in *NUT* carcinoma and interconnecting nests are characteristic of AES. Ectopic pituitary adenoma usually presents with neuroendocrine nuclear monotony and may occasionally harbor a pseudopapillary structure in the small biopsy. It is interesting to find that HMSC may sometimes demonstrate unusual acantholytic changes resembling a *DEK::AFF2* carcinoma. We recognized in this study that the defining molecular alterations in the aforementioned tumors were found to be mutually exclusive with *DEK* rearrangement. In difficult cases, ancillary IHC for AFF2 as well as p16, INI1, *NUT*, *NKX2.2*, synaptophysin, etc. would be helpful for diagnosis.

In conclusion, *DEK::AFF2* fusion was identified in 10.7% (3/28) of consecutive samples of SPs and sinonasal SCCs using publicly

available RNAseq data. *AFF2* gene expression was significantly higher in the fusion-positive cases compared to the wild-type tumors ( $p < 0.001$ ), while no significant differences in *DEK* gene expression were noted. The majority of *DEK::AFF2* carcinomas is morphologically low-grade with histologic similarity to other sinonasal tumors with predominantly papillary growth. The IHC assay using an anti-AFF2 C-terminus antibody is a highly sensitive and specific ancillary marker that distinguishes *DEK::AFF2* carcinomas from the other sinonasal tumors with overlapping morphological features.

#### DATA AVAILABILITY

The data that support the findings of this study are available from the corresponding author upon reasonable request.

#### REFERENCES

- Yang, W., Lee, K.W., Srivastava, R.M., Kuo, F., Krishna, C., Chowell, D. et al. Immunogenic neoantigens derived from gene fusions stimulate T cell responses. *Nat. Med.* **25**, 767–775 (2019).
- Todorovic, E., Truong, T., Eskander, A., Lin, V., Swanson, D., Dickson, B.C. et al. Middle ear and temporal bone nonkeratinizing squamous cell carcinomas with *DEK-AFF2* fusion: an emerging entity. *Am. J. Surg. Pathol.* **44**, 1244–1250 (2020).
- Bishop, J.A., Gagan, J., Paterson, C., McLellan, D., Sandison, A. Nonkeratinizing Squamous Cell Carcinoma of the Sinonasal Tract With *DEK-AFF2*: Further Solidifying an Emerging Entity. *Am. J. Surg. Pathol.* **45**, 718–720 (2021).
- Kuo, Y.J., Lewis, J.S., Jr, Zhai, C., Chen, Y.A., Chernock, R.D., Hsieh, M.S. et al. *DEK-AFF2* fusion-associated papillary squamous cell carcinoma of the sinonasal tract: clinicopathologic characterization of seven cases with deceptively bland morphology. *Mod. Pathol.* **34**, 1820–1830 (2021).
- Rooper LM, Agaimy A, Dickson BC, Dueber JC, Eberhart CG, Gagan J, et al. *DEK-AFF2* Carcinoma of the Sinonasal Region and Skull Base: Detailed Clinicopathologic Characterization of a Distinctive Entity. *Am. J. Surg. Pathol.* **45**, 1682–1693 (2021).
- Waldmann, T., Scholten, I., Kappes, F., Hu, H.G., Knippers, R. The *DEK* protein—an abundant and ubiquitous constituent of mammalian chromatin. *Gene* **343**, 1–9 (2004).
- Riveiro-Falkenbach, E., Soengas, M.S. Control of tumorigenesis and chemoresistance by the *DEK* oncogene. *Clin. Cancer Res.* **16**, 2932–2938 (2010).
- Teng, Y., Lang, L., Jauregui, C.E. The Complexity of *DEK* Signaling in Cancer Progression. *Curr. Cancer Drug Targets* **18**, 256–265 (2018).
- Ishida, K., Nakashima, T., Shibata, T., Hara, A., Tomita, H. Role of the *DEK* oncogene in the development of squamous cell carcinoma. *Int. J. Clin. Oncol.* **25**, 1563–1569 (2020).
- Wise-Draper, T.M., Draper, D.J., Gutkind, J.S., Molinolo, A.A., Wikenheiser-Brokamp, K.A., Wells, S.I. Future directions and treatment strategies for head and neck squamous cell carcinomas. *Transl. Res.* **160**, 167–177 (2012).
- Adams, A.K., Hallenbeck, G.E., Casper, K.A., Patil, Y.J., Wilson, K.M., Kimple, R.J., et al. *DEK* promotes HPV-positive and -negative head and neck cancer cell proliferation. *Oncogene* **34**, 868–877 (2015).



12. Nakashima, T., Tomita, H., Hirata, A., Ishida, K., Hisamatsu, K., Hatano, Y. et al. Promotion of cell proliferation by the proto-oncogene DEK enhances oral squamous cell carcinogenesis through field cancerization. *Cancer Med.* **6**, 2424–2439 (2017).
13. Bensaid, M., Melko, M., Bechara, E.G., Davidovic, L., Berretta, A., Catania, M.V. et al. FRAXE-associated mental retardation protein (FMR2) is an RNA-binding protein with high affinity for G-quartet RNA forming structure. *Nucleic Acids Res.* **37**, 1269–1279 (2009).
14. Ge, H., Liu, K., Juan, T., Fang, F., Newman, M., Hoeck, W. FusionMap: detecting fusion genes from next-generation sequencing data at base-pair resolution. *Bioinformatics* **27**, 1922–1928 (2011).
15. Robinson, J.T., Thorvaldsdottir, H., Wenger, A.M., Zehir, A., Mesirov, J.P. Variant Review with the Integrative Genomics Viewer. *Cancer Res.* **77**, e31–e34 (2017).
16. Dobin, A., Davis, C.A., Schlesinger, F., Drenkow, J., Zaleski, C., Jha, S., et al. STAR: ultrafast universal RNA-seq aligner. *Bioinformatics* **29**, 15–21 (2013).
17. Anders, S., Pyl, P.T., Huber, W. HTSeq-a Python framework to work with high-throughput sequencing data. *Bioinformatics* **31**, 166–169 (2015).
18. Bell, D., Bell, A.H., Kupferman, M.E., Prieto, V.G., Weber, R.S., Hanna, E.Y. Comparative transcriptome analysis of sinonasal inverted papilloma and associated squamous cell carcinoma: Out-HOXing developmental genes. *Head Neck* **41**, 3090–3104 (2019).
19. Saab-Chalhoub, M.W., Guo, X., Shi, Q., Chernock, R.D., Lewis, J.S., Jr Low Grade Papillary Sinonasal (Schneiderian) Carcinoma: A Series of Five Cases of a Unique Malignant Neoplasm with Comparison to Inverted Papilloma and Conventional Nonkeratinizing Squamous Cell Carcinoma. *Head Neck Pathol.* **15**, 1221–1234 (2021).
20. Lewis, J.S., Jr., Chernock, R.D., Haynes, W., El-Mofty, S.K. Low-grade papillary schneiderian carcinoma, a unique and deceptively bland malignant neoplasm: report of a case. *Am. J. Surg. Pathol.* **39**, 714–721 (2015).
21. Zhai, C., Wang, H., Li, S., Wang, D. Clinicopathological analysis of low-grade papillary Schneiderian carcinoma: report of five new cases and review of the literature. *Histopathology* **79**, 370–380 (2021).
22. Bishop, J.A., Brandwein-Gensler, M., Nicolai, P., Steens, S., Syjanen, S., Westra, W.H. Non-keratinizing squamous cell carcinoma, (eds El-Naggar, A.K., Chan, J.K.C., Grandis, J.R., Takata, T., Sliotweg, P.J.). *WHO Classification of Head and Neck Tumours*. 4th edn. 15–17 (IARC: Lyon, 2017).
23. Bishop, J.A., Guo, T.W., Smith, D.F., Wang, H., Ogawa, T., Pai, S.I. et al. Human papillomavirus-related carcinomas of the sinonasal tract. *Am. J. Surg. Pathol.* **37**, 185–192 (2013).
24. El-Mofty, S.K., Lu, D.W. Prevalence of high-risk human papillomavirus DNA in nonkeratinizing (cylindrical cell) carcinoma of the sinonasal tract: a distinct clinicopathologic and molecular disease entity. *Am. J. Surg. Pathol.* **29**, 1367–1372 (2005).
25. Larque, A.B., Hakim, S., Ordi, J., Nadal, A., Diaz, A., del Pino, M., et al. High-risk human papillomavirus is transcriptionally active in a subset of sinonasal squamous cell carcinomas. *Mod. Pathol.* **27**, 343–351 (2014).
26. Nudell, J., Chiosea, S., Thompson, L.D. Carcinoma ex-Schneiderian papilloma (malignant transformation): a clinicopathologic and immunophenotypic study of 20 cases combined with a comprehensive review of the literature. *Head Neck Pathol.* **8**, 269–286 (2014).
27. Bubola, J., MacMillan, C.M., Weinreb, I., Witterick, I., Swanson, D., Zhang, L., et al. A Poorly Differentiated Non-keratinizing Sinonasal Squamous Cell Carcinoma with a Novel ETV6-TNFRSF8 Fusion Gene. *Head Neck Pathol.* **15**, 1284–1288 (2021).
28. Agaimy, A., Hartmann, A., Antonescu, C.R., Chiosea, S.I., El-Mofty, S.K., Geddert, H. et al. SMARCB1 (INI-1)-deficient Sinonasal Carcinoma: A Series of 39 Cases Expanding the Morphologic and Clinicopathologic Spectrum of a Recently Described Entity. *Am. J. Surg. Pathol.* **41**, 458–471 (2017).
29. French, C.A. NUT Carcinoma: Clinicopathologic features, pathogenesis, and treatment. *Pathol. Int.* **68**, 583–595 (2018).
30. Bishop, J.A., Alaggio, R., Zhang, L., Seethala, R.R., Antonescu, C.R. Adamantinoma-like Ewing family tumors of the head and neck: a pitfall in the differential diagnosis of basaloid and myoepithelial carcinomas. *Am. J. Surg. Pathol.* **39**, 1267–1274 (2015).

## ACKNOWLEDGEMENTS

The authors would like to thank the Biobank, Taipei Veterans General Hospital for assistance with sample preparation in this study. This study was presented in part at the annual meeting of the United States and Canadian Academy of Pathology on March 21st, 2022, Los Angeles, CA, USA.

## AUTHOR CONTRIBUTIONS

Y.J.K. and J.F.H. performed the study concept and design, analyzed the data, and wrote the paper; Y.C.Y. and J.F.H. conducted bioinformatics analysis of the RNAseq data; Y.J.K., J.S.L., T.T., R.D.C., C.Z., Y.A.C., T.H., C.K.L., Q.S., J.M.V., A.B.G., Y.H.C., M.S.H., A.H., and J.F.H. provided specimen acquisition and clinical data; J.F.H. supported immunohistochemistry and molecular methodology; J.S.L., R.D.C., and I.W. performed critical review and editing. All authors read and approved the final paper.

## FUNDING

The study was supported by the research grants from Taipei Veterans General Hospital (V110B-019) and the Ministry of Science and Technology, Taiwan (MOST110-2320-B-075-003-MY3).

## COMPETING INTERESTS

The authors declare no competing interests.

## ETHICS APPROVAL AND CONSENT TO PARTICIPATE

The study was approved by the institutional review board (IRB) of Taipei Veterans General Hospital (IRB no.: 2020-12-012CC).

## ADDITIONAL INFORMATION

**Supplementary information** The online version contains supplementary material available at <https://doi.org/10.1038/s41379-022-01117-4>.

**Correspondence** and requests for materials should be addressed to Jen-Fan Hang.

**Reprints and permission information** is available at <http://www.nature.com/reprints>

**Publisher's note** Springer Nature remains neutral with regard to jurisdictional claims in published maps and institutional affiliations.